Annals of Lung Cancer Research

Case Report
Published: 14 Aug, 2020

The Positron Emission Tomography Scan for Primary Pulmonary Primitive Neuroectodermal Tumor: A Case Report and Literature Review

Sezgi Şahin Duyar[1], Özlem Sönmez[1], Tuğba Nur Tezvergil[1], Dicle Kaymaz[1], Nesrin Gürçay[2] and Füsun Ardıç Yükrük[3]*

[1]Department of Chest Diseases, Ankara Atatürk Chest Diseases and Thoracic Surgery Education and Research Hospital, Turkey

[2]Department of Pathology, Ankara Atatürk Chest Diseases and Thoracic Surgery Education and Research Hospital, Turkey

[3]Department of Pathology, Ankara Dr Abdurrahman Yurtaslan Oncology Training and Research Hospital, Turkey

Abstract

Primitive neuroectodermal tumors which known as highly aggressive ones, commonly originated from the bone and soft tissues of children or young adults. This tumor group that stems from lung parenchyma is an exceptional case. We report a case of a 20-years old man with pulmonary primitive neuroectodermal tumor. The positron emission tomography scan findings of this rare disease were summarized.

Keywords: Lung; Peripheral; Positron emission tomography; Young adult; Primitive neuroectodermal tumor

OPEN ACCESS

Correspondence:
Tuğba Nur Tezvergil, Department of Chest Diseases, Ankara Atatürk Chest Diseases and Thoracic Surgery Education and Research Hospital, Sanatoryum Avenue, Keçiören, Ankara, Turkey, Tel: +905469347392; Fax: +903123552135; E-mail: tugbanurtezvergil@outlook.com

Received Date: *20 Jul 2020*
Accepted Date: *11 Aug 2020*
Published Date: *14 Aug 2020*

Citation:
Duyar SŞ, Sönmez Ö, Tezvergil TN, Kaymaz D, Gürçay N, Yükrük FA. The Positron Emission Tomography Scan for Primary Pulmonary Primitive Neuroectodermal Tumor: A Case Report and Literature Review. Ann Lung Cancer Res. 2020; 1(1): 1001.

Abbreviations

PNET: Primitive Neuroectodermal Tumors; pPNET: peripheral Primitive Neuroectodermal Tumors; MTB/RIF: Mycobacterium Tuberculosis/Rifampicin; CT: Computed Tomograpy; 18F-FDG PET-CT: 18-Fluorodeoxyglucose Positron Emission Tomography; SUV: Standardized Uptake Value; Bcl-2: B-cell lymphoma 2; PAS: Periodic Acid-Schiff; NSE: Neuron-Specific Enolase; TTF-1: Thyroid Transcription Factor-1; ERG: ETS-Related Gene; FLI-1: Friend Leukemia Integration-1

Introduction

PNETs outside the central nervous system are called peripheral PNETs. Unlike ordinary PNET cases of the chest wall, pelvic bones, and extremities; PNET of the lung parenchyma without chest wall involvement is quite rare [1].

Case Presentation

A 20-years old male patient admitted to our clinic with complaints of cough, hemoptysis, weight loss, and pleuritic chest pain. He had lost five kilograms in the past year. He declared a smoking history of 1.5 packs/year and three-four times of marijuana usage in the last two years. There were no other symptoms suggestive of any other organs involvement. Physical examination revealed the diminution of breathing sounds on the left hemithorax below the scapula.

The radiologic evaluation of the chest X-ray indicated homogeneous opacity in the lower zone of the left lung, non-homogeneous opacities in the right upper zone, and right hilar enlargement (Figure 1). The laboratory test resulted as follows: WBC: 7070/µL, HGB: 11.5 g/dl, ALT: 107 IU/L, AST: 96 IU/L, CRP: 293 mg/dl, and sedimentation: 106 mm/h. The sputum smear analyzed with Xpert MTB/RIF and acid-fast staining were negative. CT scan of the chest revealed 15 cm sized mass with pleural effusion in the left hemithorax, multiple pulmonary lesions on the right lung (the largest one is 6.8 cm in diameter) with multiple mediastinal lymphadenopathies (Figure 2). The initial non-specific antibiotheraphy with ceftriaxone and metronidazole did not yield any clinical or radiological response. Pleural fluid was too minimal to sample by thorax ultrasonography. Due to suspicion for malignancy the patient underwent 18FDG PET-CT scan. Hypermetabolic activity was observed in the lesions of the both lungs (SUVmax: 6.9 for the 15 cm sized mass on the left lower

Table 1: PET scan results of pulmonary pPNET patients reported in the literatures.

Year	Sex	Age	Number of Cases	Location	Size (cm)	SUV (max)	Ref.
2009	F	73	1	LLL	7	4.36	Kara Gedik G et al. [14]
2009	M	17	1	RUL	10	8.3	Demir MK et al. [15]
2010	M	18	1	RUL/M	NS	NS	Kamaleswaran et al. [16]
2014	M/F	15*	6	CW/M	5.1-13.7	4-18.6	Xia et al. [6]
2015	M	16	1	BMN	0.5-1	NS	Dong M et al. [1]
2017	M	58	1	RLL	7.7	17.2	Başgöz BB et al. [5]
2019	M	28	1	LUL	2.8	NS	Ekin S et al. [7]

SUV: Standardized Uptake Value; F: Female; M: Male; LLL: Left Lower Lobe; RUL: Right Upper Lobe; M: Mediastinum; CW: Chest Wall; BMN: Bilateral Multiple Nodules; RLL: Right Lower Lobe; LUL: Left Upper Lobe; NS: Not Stated; Ref: References; *: mean

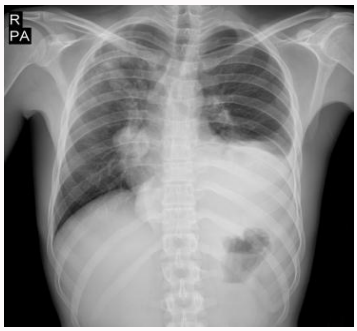

Figure 1: Chest X-ray: Nonhomogeneous opacities on the left lung lower zone, approximately 3 cm × 4 cm sized mass on the middle zone of the right lung.

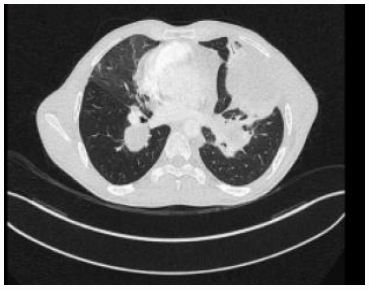

Figure 2: Thorax CT: 15 cm sized mass on the left hemithorax and 5 cm sized central mass on the right hemithorax.

lobe, SUVmax: 3.69 for 5.5 cm sized mass on the right lower lobe and SUVmax: 3.03 for 2.2 cm sized nodular lesion in the right upper lobe). The millimetric nodules on the left upper lobe did not show any hypermetabolic activity. In the mediastinum, right paratracheal, aorticopulmonary, left parasternal, prevascular, subcarinal, left hilar (SUVmax: 2.70), right hilar (SUVmax: 4.86), and left supraphrenic lymph nodes had mildly increased 18F-FDG uptake. Due to the absence of endobronchial lesion on fiberoptic bronchoscopy, CT-guided transthoracic tru-cut biopsy was applied to the mass on the left lung. Histopathological examination of the sections exposed small, round, and blue tumor cells which is the common morphology of PNET. The immunohistochemical staining was positive for Bcl-2 and PAS. Ki-67 proliferation index was found as 10%. The lack of CD45 immune-positivity ruled out lymphoma in differential diagnosis. CD56, synaptophysin, chromogranin, NSE, and TTF-1 were all negative. The final diagnosis of pPNET originated from lung parenchyma was reached after the further immunohistochemical and cytogenetic evaluation which resulted in positivity for CD99, Fli1, and ERG.

Table 2: PET scan findings of the case.

Location	Size (cm)	SUVmax
Left lower lobe	15	6.9
Right lower lobe	5.5	3.69
Right upper lobe	2.2	3.03
Left upper lobe	0.8	not stated

Discussion

PNETs are highly aggressive tumors of the soft tissues and skeletal system [2]. In 1918, Stout et al. [3] discovered this tumor group in the ulnar nerve of an adult patient. In 1979, Askin et al. [4] published a series of cases reporting PNETs placed in thoracopulmonary region which diagnosed at twenty patients whose age average is fourteen. After some recent studies pointed out the similar genetic features of Ewing Sarcoma, extraosseous Ewing Sarcoma, and PNET, these tumors were classified as "Ewing Sarcoma Family of Tumors." Clinical symptoms of pulmonary PNETs may vary including cough, chest pain, hemoptysis, and shortness of breath. As in our case, PNETs are commonly seen in young male patients [5]. The radiologic presentation of primitive pulmonary PNETs tends to be large masses on CT scan [6,7]. However, in this case, rapidly growing nature of this tumor caused a "giant" mass with 15 cm in size, which is probably the largest PNET in the literature. The bilateral lung metastasis and mediastinal involvement also contribute to the rarely seen presentation of this case.

Recently published case reports and case series indicated that PET scan may be useful in the diagnosis and follow-up of patients with pPNET. Györke et al. [8] found that PET is more sensitive than bone scintigraphy for the bone metastases of Ewing tumors. In this study the mean SUV of the true-positive cases was 4.54 ± 2.79. Another study recommended the guidance of the elevated SUV max for evaluation of the bone marrow involvement in the patients with Ewing tumors instead of blind bone marrow aspiration [9]. Avoiding bone marrow aspiration was also suggested for the patients who do not have any distant metastasis on ^{18}F-FDG PET-CT [10]. An increased ^{18}F-FDG activity in PET-CT was reported in the cases with kidney, ileum originated PNETs as well [11,12]. However, the soft tumor of the forearm diagnosed as pPNET did not cause any increase in FDG uptake [13]. The metabolic features of pPNET according to the origins of the tumors must be further investigated.

The PET scan findings of the pulmonary pPNETS in the literature are summarized in Table 1. Out of 12 cases reported since 2009, only one case with multiple small nodules lacked hypermetabolic activity on PET scan [1,5-7,14-16]. The data on Table 1 and PET scan findings

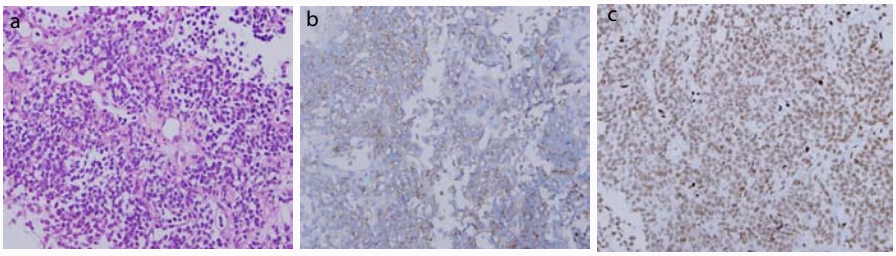

Figure 3a: Neoplastic cells staining with H&E (400x). **3b:** Neoplastic cells showing immunoreactivity with CD99 **3c:** Neoplastic cells showing immunoreactivity with Fli1.

of our case (Table 2) implicate a possible correlation of tumor size and SUVmax. It can be speculated that SUVmax increases with the size of the lesion for pulmonary pPNETS. This hypothesis must be statistically evaluated.

The pathologic diagnosis of PNET is based on the classical morphology of small, blue, and round cells with scant cytoplasm, hyperchromatic nucleus, and necrosis on the light microscopy. Furthermore, immunohistochemical studies for specific neural differentiation markers such as CD99, S100, neuron specific enolase, vimentin, synaptophysin, chromogranin must be used for differential diagnosis. PAS could be found positive in some cases. PNETs should be negative for markers for epithelial, lymphoid, smooth/skeletal muscle and melanoma [5,17]. PNET/ESFT is specifically characterized by balanced reciprocal translocations. While 85% of the cases have EWS/Fli1 fusion genes constituted by t (11;22) (q24;q22), the others mostly have EWS/ERG fusion genes which is constituted by t(21;22) [18,19]. Our case was positive with PAS, CD99 and EWS/Fli1 and EWS/ERG.

Although it is quite rare, a large tumor in the lung with moderate SUV on PET-CT should raise suspicion for pulmonary pPNET during differential diagnosis especially for a young male patient. Beside the major role of immunohistochemical studies for the diagnosis, 18FDG PET-CT is also beneficial for the diagnostic approach and the treatment choice. Our case was not suitable for the surgical resection because of the metastatic lesions both of the lungs which were evident on the PET scan. We referred the patient to medical oncology department for chemotherapy.

Conclusion

We presented this rare case who has a unique radiologic appearance of a giant pulmonary mass with multiple intrathoracic metastatic lesions and outlined the recent data on PET scan findings of pulmonary pPNET and the diagnostic approach for this disease.

References

1. Dong M, Liu J, Song Z, Li X, Shi T, Wang D, et al. Primary multiple pulmonary primitive neuroectodermal tumor: Case report and literature review. Medicine (Baltimore). 2015;94(27):e1136.
2. Batsakis JG, Mackay B, el-Naggar AK. Ewing's sarcoma and peripheral primitive neuroectodermal tumor: An interim report. Ann Otol Rhinol Laryngol. 1996;105(10):838-43.
3. Stout AP. A tumor of the ulnar nerve. Proc NY Pathol Soc. 1918;18:2-12.
4. Askin FB, Rosai J, Sibley RK, Dehner LP, McAlister WH. Malignant small cell tumor of the thoracopulmonary region in childhood: A distinctive clinicopathologic entity of uncertain histogenesis. Cancer. 1979;43(6):2438-51.
5. Başgöz BB, Aydin A, Ince S, Demirci I, Özcan A. Late onset of primary pulmonary primitive neuroectodermal tumor: A case report. Clujul Med. 2017;90(4):449-52.
6. Xia T, Guan Y, Chen Y, Li J. Askin tumor: CT and FDG-PET/CT imaging findings and follow-up. Medicine (Baltimore). 2014;93(6):e42.
7. Ekin S, Çobanoğlu U, Göya C, Erten R, Yıldız H. Ewing's sarcoma of the lung: A rare case. Tuberk Toraks. 2019;67(2):146-8.
8. Györke T, Zajic T, Lange A, Schäfer O, Moser E, Makó E, et al. Impact of FDG PET for staging of Ewing sarcomas and primitive neuroectodermal tumours. Nucl Med Commun. 2006;27(1):17-24.
9. Kasalak Ö, Glaudemans AWJM, Overbosch J, Jutte PC, Kwee TC. Can FDG-PET/CT replace blind bone marrow biopsy of the posterior iliac crest in Ewing sarcoma? Skeletal Radiol. 2018;47(3):363-7.
10. Inagaki C, Shimoi T, Okuma HS, Kawachi A, Sudo K, Shimomura A, et al. Bone marrow examination in patients with Ewing sarcoma/peripheral primitive neuroectodermal tumor without metastasis based on 18F-fluorodeoxyglucose positron emission tomography/computed tomography. Med Oncol. 2019;36(7):58.
11. Yu P, Xiaochun F, Jing L, Yifan Z. Rare Ileal Ewing sarcoma/primitive neuroectodermal tumor on 18F-FDG PET/CT. Clin Nucl Med. 2017;42(10):809-11.
12. Tripathy S, Shamim SA, Chellapuram S, Barwad A, Rastogi S. Primary Ewing sarcoma/primitive neuroectodermal tumor of kidney with inferior vena cava thrombus: Findings on 18F-FDG PET/CT. Clin Nucl Med. 2020;45(2):e103-5.
13. Musana KA, Raja S, Cangelosi CJ, Lin YG. FDG PET scan in a primitive neuroectodermal tumor. Ann Nucl Med. 2006;20(3):221-5.
14. Gedik GK, Sari O, Altinok T, Tavli L, Kaya B, Kara PO. Askin's tumor in an adult: Case report and findings on 18F-FDG PET/CT. Case Rep Med. 2009;2009:517329.
15. Demir MK, Koşar F, Sanli Y, Esmaeilzadeh S, Urer HN. 18F-FDG PET-CT features of primary primitive neuroectodermal tumor of the chest wall. Diagn Interv Radiol. 2009;15(3):172-5.
16. Kamaleshwaran KK, Mittal BR, Chakraborty D, Bhattacharya A, Gupta N, Jindal SK, et al. Imaging with 18F-FDG PET/CT of a primitive primary neuroectodermal tumor of the chest wall, in an adult. Hell J Nucl Med. 2010;13(3):287-8.
17. Pinto A, Dickman P, Parham D. Pathobiologic markers of the Ewing sarcoma family of tumors: State of the art and prediction of behaviour. Sarcoma. 2011;2011:856190.
18. Elzi DJ, Song M, Houghton PJ, Chen Y, Shiio Y. The role of FLI-1-EWS, a fusion gene reciprocal to EWS-FLI-1, in Ewing sarcoma. Genes Cancer. 2015;6(11-12):452-61.
19. Andrei M, Cramer SF, Kramer ZB, Zeidan A, Faltas B. Adult primary pulmonary primitive neuroectodermal tumor: Molecular features and translational opportunities. Cancer Biol Ther. 2013;14(2):75-80.